

# Comparative Analysis of Speed and Position Control of BLDC Motor via Field Oriented Control Using SPWM and SVPWM Schemes

Sanjan P S<sup>1</sup>, Dr. Madhu B R<sup>2</sup>

<sup>1</sup>Department of Electrical and Electronics, RV College of Engineering, Bangalore, India

<sup>2</sup>Assistant Professor, Department of Electrical and Electronics, RV College of Engineering, Bangalore, India

\*\*\*

**Abstract**— In this paper, a comparative analysis is carried out on the performance of a Field Oriented Controlled (FOC) based speed and position control of BLDC motor using Sinusoidal Pulse Width Modulation (SPWM) and Space Vector Pulse Width Modulation (SVPWM) schemes. FOC is commonly used in high performance motor driver/controller for its superior performance such as high efficiency and lower torque ripple content, especially in applications such as robotics, electric vehicles, power tools, etc. Advancements in Digital Signal Processors and lower costs have allowed this technique to be used in more high-performance applications. The overall performance also depends on PWM control scheme used. SPWM and SVPWM techniques are two most commonly used techniques in motor control and inverter control applications. Hence a comparison study is carried out with the two schemes using Simulink. In light loading conditions, the results show that the performance is quite similar, but on closer inspection, SVPWM based FOC offers better performance compared to SPWM based FOC.

**Keywords**—FOC; BLDC; SVPWM; SPWM; Clarke Transformation; Park Transformation;

## I. INTRODUCTION

Over the years, Brushless DC Motors (BLDC), a type of permanent magnet synchronous motor has gained wide spread popularity. Now, it is commonly used in electric vehicles, precision motor control applications such as CNCs and robotic arms, power tools, aerospace applications, drones etc. This is due to its high-power density, high efficiency, more robust and reliable compared to a typical brushed DC motor, also, high rotor speeds can be achieved and quieter operation. Typical construction of a BLDC motor uses an armature that is stationary with the three phase coils arranged 120° electrical apart and permanent magnets are attached on the rotor. Due to this type of construction, the commutation needs to be done electronically unlike a brushed DC motor that commutates mechanically. In order to control a BLDC motor, the current flowing through each coil needs to be controlled, by doing so, the net magnetic field vector can be controlled (i.e., both direction of rotation and magnitude). The rotor magnetic field catches up with the net stator magnetic field vector to produce torque, since the strength of magnetic field is directly dependent on the current flowing in the coils, the torque can be controlled [1-3].

Various BLDC control techniques have been defined in literature, these include, trapezoidal control that involves controlling the current through any two pair of coils

simultaneously, the sequence of firing is decided by a lookup table and feedback from the hall effect sensors that measure rotor position. Although this technique is simple to implement, it does not provide smooth and precise motor control. Sinusoidal control involves controlling the three phase currents though the coils sinusoidally as the motor rotates. This results in a smoothly rotating magnetic field vector; therefore, it eliminates the torque ripples and commutation spikes. One of the drawbacks with this technique is that its performance degrades at higher speeds because of the time variant nature of the control scheme that causes the breakdown due to limited bandwidth of PI (Proportional Integral) Controller. Field-oriented control, also called as vector control is a scheme that offers great performance and efficiency. In this technique, the stator currents of the motor are represented in dq reference frame. One vector corresponds to the magnetic flux of the rotor and the other vector represents the torque. By manipulating these vectors based on the desired output required, the motor is controlled. A detailed explanation of this scheme is provided in section. Although this scheme requires high processing requirements, recent advancements and reduction of cost in microprocessor and power electronics technology have led to wide spread usage of this scheme in AC motor drives [2-3].

For field-oriented control and various other industrial application, two of the most commonly used PWM (Pulse Width Modulation) schemes to control the inverter are SPWM (Sinusoidal PWM) and SVPWM (Space Vector PWM). In SPWM technique, two different signal types are used – sinusoidal reference waveforms and a high frequency triangular waveform (i.e., carrier waveform) for comparison to generate pulses. In SVPWM, the rotating space vector of either the reference voltage or current is recomposed by taking the vector sum of available base vectors [5-8].

Position control requires feedback of the rotor position, usually encoders are used to sense the rotor position. There are various types of encoders such as magnetic and optical encoders, in this there are incremental and absolute types. Depending on the application and accuracy it demands an appropriate encoder is selected. An encoder can provide information on direction of rotation, speed, amount of rotation and position. The sensitivity of an encoder is defined by its resolution. In general, a typical FOC based speed and position control is shown in Fig. 1. It consists of three control loops. Position control loop feeds the speed control loop, this inturn feeds the current control loop [9-12].

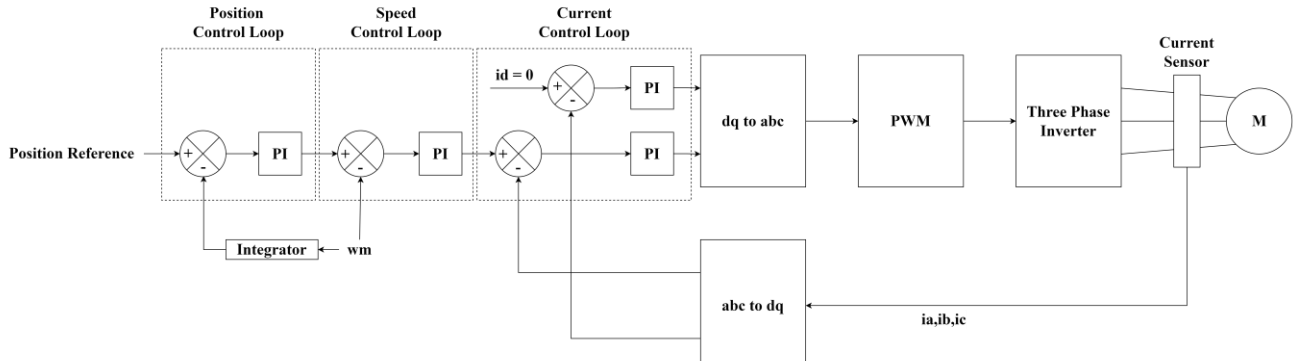


Fig. 1. General Block Diagram of Position and Speed Control of BLDC Motor Using FOC

## II. MODELLING OF THE BLDC MOTOR

Let's assume a system of BLDC motor connected via a three-phase inverter and powered by a DC source as shown in Fig.2. To model the motor, consider a star connected configuration for the BLDC motor [2] and assuming a balanced three phase system, then,  $R = R_a + R_b + R_c$ .

$$V_a = RI_a + (L - M) \frac{dI_a}{dt} + e_a \quad (1)$$

$$V_b = RI_b + (L - M) \frac{dI_b}{dt} + e_b \quad (2)$$

$$V_c = RI_c + (L - M) \frac{dI_c}{dt} + e_c \quad (3)$$

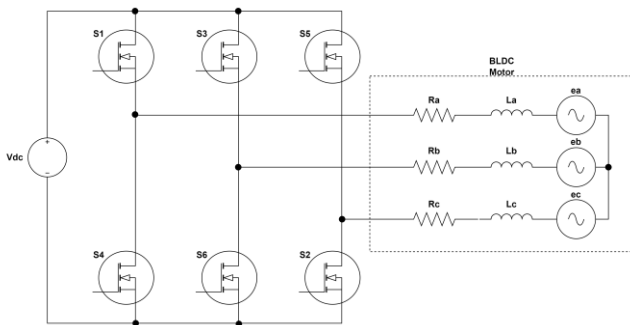


Fig. 2. Equivalent Circuit of BLDC Motor

In equation (1-3),

$V_a, V_b, V_c$  = phase voltages

$R$  = Armature resistance

$L$  = Armature self-inductance

$M$  = Mutual inductance

$I_a, I_b, I_c$  = phase current

$E_a, E_b, E_c$  = motor back emf

The back emf of the motor is written as shown in (4-7)-

$$e_a = K_w f(\theta_e) \omega \quad (4)$$

$$e_b = K_w f(\theta_e - \frac{2\pi}{3}) \omega \quad (5)$$

$$e_c = K_w f(\theta_e + \frac{2\pi}{3}) \omega \quad (6)$$

$$f = \begin{cases} 1 & 0 \leq \theta_e \leq \frac{2\pi}{3} \\ 1 - \frac{6}{\pi}(\theta_e - \frac{2\pi}{3}) & \frac{2\pi}{3} \leq \theta_e \leq \pi \\ -1 & \pi \leq \theta_e \leq \frac{5\pi}{3} \\ -1 - \frac{6}{\pi}(\theta_e - \frac{5\pi}{3}) & \frac{5\pi}{3} \leq \theta_e \leq 2\pi \end{cases} \quad (7)$$

The electrical angle,  $\theta_e = (P/2)\theta_m$ , where  $\theta_m$  is the mechanical angle of the rotor and  $P$  are the number of pole pairs. The function given by  $f$  in (7) gives the back emf that is trapezoidal in nature for phase A of the motor.  $K_w$  is the back emf constant and  $\omega$  is the rotor speed.

The electromagnetic torque in both electrical form and mechanical form is given in (8) and (9) respectively.

$$T_{em} = \frac{1}{\omega} (e_a i_a + e_b i_b + e_c i_c) \quad (8)$$

$$T_e = J \frac{d\omega}{dt} + B\omega + T_L \quad (9)$$

In this,

$P$  = Number of pole pairs

$T_L$  = Load Torque

$J$  = Moment of Inertia

$B$  = Friction Constant

## III. FIELD ORIENTED CONTROL

Fig.3 shows the vector representation of the stator current in abc, alpha-beta and dq reference frames. For conversion from abc to alpha-beta reference frame, only two instantaneous current vectors are sufficient, in this case phase currents of a and b. Phase c current can be computed using the current relation shown in (10).

$$i_a + i_b + i_c = 0 \quad (10)$$

Using Clarke's transformation, the phase vectors are converted to alpha-beta orthogonal reference frame (11-12).

$$i_\alpha = i_a \quad (11)$$

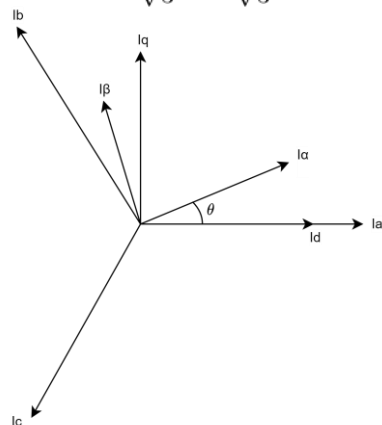
$$i_{\beta} = \frac{1}{\sqrt{3}}i_a + \frac{2}{\sqrt{3}}i_b \quad (12)$$


Fig. 3. Current Vector Representation Combined

Using Park's transformation, the vectors are converted from alpha-beta coordinate system to dq coordinate system (13-14).

$$i_d = i_{\alpha} \cos(\theta) + i_{\beta} \sin(\theta) \quad (13)$$

$$i_q = -i_{\alpha} \sin(\theta) + i_{\beta} \cos(\theta) \quad (14)$$

Here,  $\theta$  is the instantaneous rotor position angle, also in the dq reference frame, the quantities are time invariant. By controlling/modifying the quadrature component of the current, the torque can be controlled. By controlling the direct component, the rotor flux can be controlled.

In order to maximize torque and overall efficiency, the direct component must be ideally maintained at zero and quadrature component is generated based on torque and speed requirements. The reference values are compared with actual values and via a PI controller, the corresponding voltage is calculated. The voltage in dq reference frame is converted back to alpha-beta coordinate system using Inverse Park's transformation as shown (15-16). This is typically used to generate the gate pulses using SVPWM.

$$V_{\alpha} = V_d \cos(\theta) - V_q \sin(\theta) \quad (15)$$

$$V_{\beta} = V_d \sin(\theta) + V_q \cos(\theta) \quad (16)$$

In order to convert from alpha-beta coordinate system to abc, Inverse Clarke's transformation is used as shown (17-19). This is used to generate the SPWM for the inverter.

$$V_a = V_{\alpha} \quad (17)$$

$$V_b = -\frac{1}{2}V_{\alpha} + \frac{\sqrt{3}}{2}V_{\beta} \quad (18)$$

$$V_c = -\frac{1}{2}V_{\alpha} - \frac{\sqrt{3}}{2}V_{\beta} \quad (19)$$

#### IV. SINUSOIDAL PULSE WIDTH MODULATION

Sinusoidal Pulse Width Modulation, is one of the most commonly used technique for motor control and inverter applications. Implementation of this technique is simple and processing requirements are less. The sinusoidal reference waveforms are compared with a high frequency triangular carrier waveform to obtain the switching pulses for the respective switches.

#### V. SPACE VECTOR PULSE WIDTH MODULATION

Space Vector Pulse Width Modulation is a more advanced technique compared to the SPWM technique. The added complexity offers many advantages such as better utilization of DC bus voltage, lower harmonics and better flexibility. Fig.4 shows a space vector representation of the inverter system with six sectors. The reference vector rotates with an angular velocity against the stationary alpha-beta reference frame. By controlling the frequency and magnitude of  $v_{ref}$ , the magnitude and frequency of the corresponding fundamental component is varied [6-8]. The required output voltage of each phase is shown in (20-22).

$$V_b = V_m \cos(\omega t - 120^\circ) \quad (20)$$

$$V_a = V_m \cos(\omega t) \quad (21)$$

$$V_c = V_m \cos(\omega t + 120^\circ) \quad (22)$$

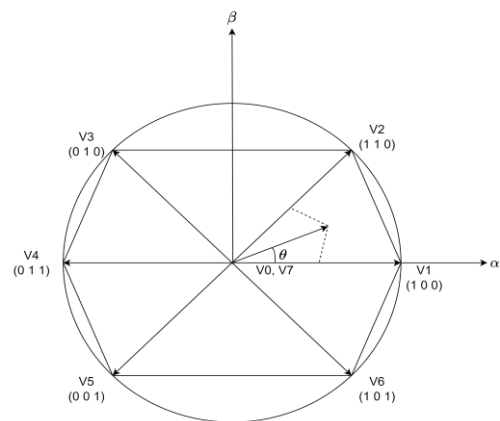


Fig. 4. Vector Representation of SVPWM

$V_{ref}$  is calculated using (23) and the Fig.5 visualizes the representation of sector 1.

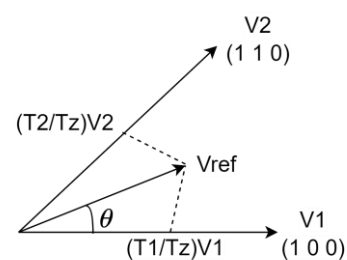


Fig. 5. Sector 1 Representation

$$V_{ref} = \sqrt{\frac{3}{2}} V_m e^{j\theta} \quad (23)$$

In this  $\theta = \omega t = 2\pi f t$

$$\vec{V}_{ref} T_Z = \vec{V}_1 T_1 + \vec{V}_2 T_2 \quad (24)$$

In this  $T_z$  is the time period of the PWM signal or the reciprocal of the switching frequency  $f_s$  (i.e.,  $T_z = 1/f_s$ ). The angle between the sectors is given by  $\phi$  with range between  $0^\circ$  to  $60^\circ$ .

$$\phi = \theta - (N - 1)60 \quad (25)$$

(26-28) is used to determine the switching period.

$$T_0 = T_Z - (T_1 + T_2) \quad (26)$$

$$T_1 = T_Z \frac{2}{\sqrt{3}} \frac{V_{ref}}{V_1} \sin(60 - \phi) \quad (27)$$

$$T_2 = T_Z \frac{2}{\sqrt{3}} \frac{V_{ref}}{V_2} \sin(\phi) \quad (28)$$

## VI. SIMULATION AND RESULTS

### A. Simulation Setup

The simulation studies are carried out using Simulink. In accordance to fig, the models for the comparison studies using the SPWM and SVPWM based speed and position control of BLDC motor is shown in Fig.6. The Simulink model consists of PMBLDC motor configured for trapezoidal back emf, stator resistance of 0.01ohms and inductance of 40uH. For the inverter, a two-level inverter block is used, powered by a DC source of 12V. The transformations are directly performed using the conversion blocks available in Simulink. The PWM scheme is directly implemented using the PWM modulator block that offers both SVPWM and SPWM capabilities. The PWM scheme is changed between studies to perform the comparison study. The switching frequency is set at 8kHz. There are three control loops, one current control loop, speed control loop and position control loop connected in cascaded configuration. In order to keep track of the

position, the integral of speed is taken. A constant torque of 0.008Nm is applied on the motor with a total simulation time of 5 seconds. Using a stair generator block, the reference position is generated. From 0, at 0.1 seconds, the position is set to 4 radians or 4 revolutions of the rotor shaft. At 2 seconds, the rotor position is set to -4 radians and is set back to 0 radians at 3.5 seconds. The PI controller of the current control loop is tuned using a separate MATLAB script. The speed and position control loop are tuned by trial-and-error method. The model is run at constant speed next to obtain the back emf and electromagnetic torque waveforms.

### B. Results

Fig.7 shows the waveforms related to the motor. In order, the first waveform shows the back emf, the phase currents and the electromagnetic torque. At the commanded positions, the waveforms using both SPWM and SVPWM look similar, upon closer inspection, the electromagnetic torque ripple is relatively less in SVPWM scheme. During position change, the current draw increases to reach the desired position, the current starts dropping once the positional error start reducing. Spikes in electromagnetic torque is seen during position changes. Fig. 8 and Fig.9 shows the comparison between speed and position waveforms respectively. The rotor speed waveforms show the speed increasing during position changes and reducing when positional error reduces. The position waveforms show the actual position and reference position waveforms. The control system is able to track the reference positions accurately and no overshoots occur. A similar conclusion is drawn by comparison of these waveforms. This similar performance is due to the light loading conditions. Fig.10 shows a comparison of the motor parameters at constant speed of 100 rad/sec with increased loading of 0.08Nm compared to the 0.008Nm previously. In this case, only a small difference is seen in the electromagnetic torque. The back-emf at this loading is at 0.7V and the current draw is close to 10A(peak). The overall torque ripple is less in SVPWM compared to SPWM. This is verified by taking a moving average of the electromagnetic torque to reduce the noise caused by switching as shown in Fig.11. There are a lot less variations in the SVPWM based FOC compared to

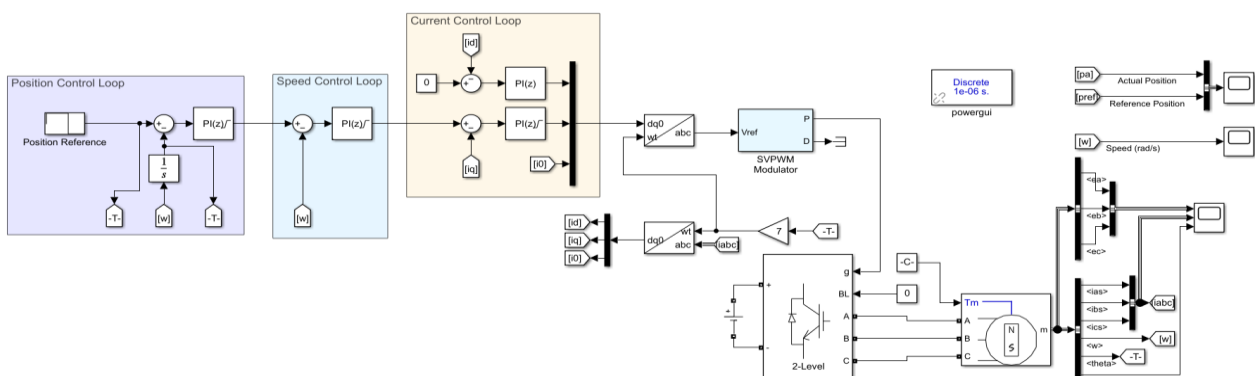


Fig. 6. Simulation Model of the FOC Based Speed and Position Control of BLDC Motor Using SPWM and SVPWM

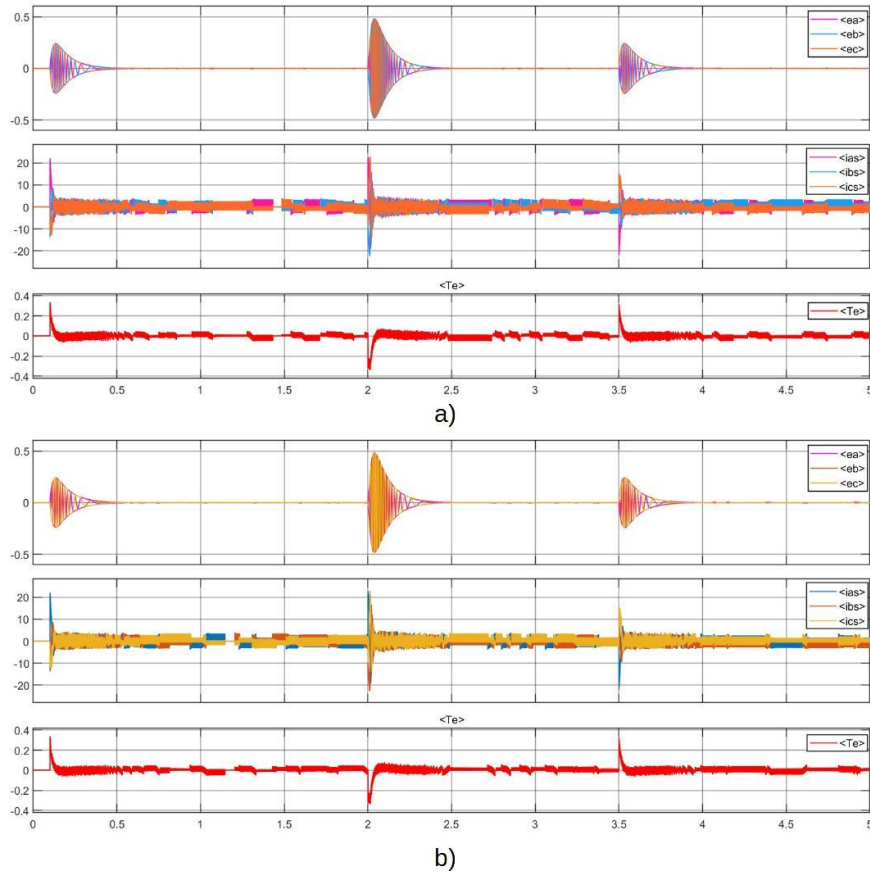


Fig. 7. Back EMF, Stator Current, Electromagnetic Torque Waveforms of the BLDC Motor a) SVPWM b) SPWM

SPWM based FOC.

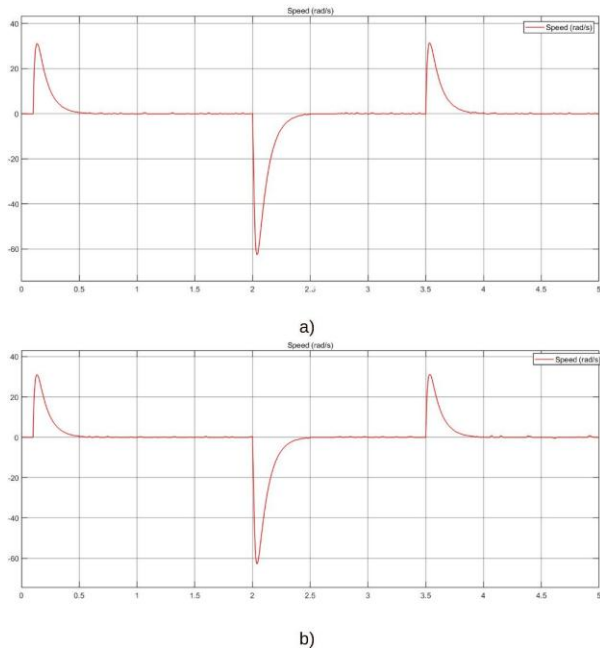


Fig. 8. Speed Waveform in rad/sec a) SVPWM b) SPWM

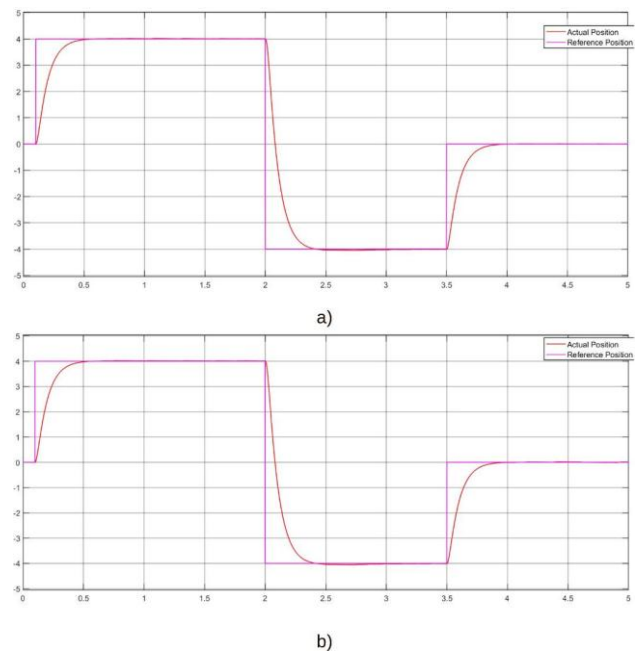


Fig. 9. Actual Position (Red) and Reference Position (Purple) Waveform a) SVPWM b) SPWM

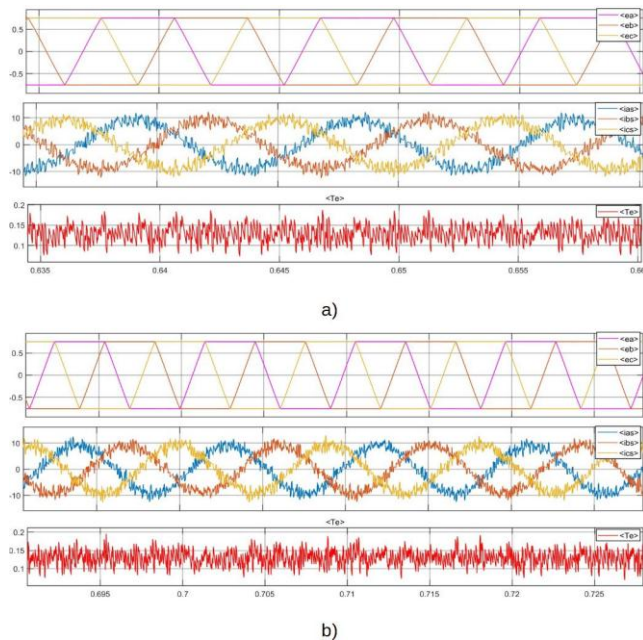


Fig. 10. Back EMF, Stator Current, Electromagnetic Torque Waveforms of the BLDC Motor at Constant Speed a) SVPWM b) SPWM

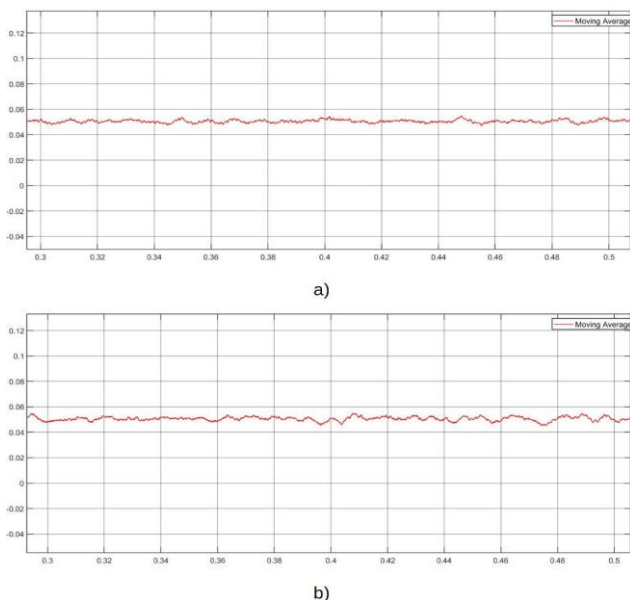


Fig. 11. Electromagnetic Torque at Constant Speed a) SVPWM b) SPWM

## VII. CONCLUSIONS

The comparison study of position and speed control of BLDC motor via FOC using SPWM and SVPWM has been carried out using Simulink and the corresponding output waveforms of comparison is presented. In this study, due to light loading conditions, the performance of the FOC based algorithm using both SPWM and SVPWM scheme are quite similar. Small variations can be seen in the waveforms especially comparing the electromagnetic torque, the

SVPWM performs slightly better with less torque ripple compared to SPWM technique. The averaged torque waveform of SVPWM is relatively smoother compared to SPWM.

## REFERENCES

- [1] Bimal K. Bose, "Modern Power Electronics and AC Drives," 2008
- [2] Gujjar, Meghana N., and Pradeep Kumar. "Comparative analysis of field oriented control of BLDC motor using SPWM and SVPWM techniques." In 2017 2nd IEEE International Conference on Recent Trends in Electronics, Information & Communication Technology (RTEICT), pp. 924-929. IEEE, 2017.
- [3] Kiran, Yadu, and Dr PS Puttaswamy. "A review of brushless motor control techniques." International Journal of Advanced Research in Electrical, Electronics and Instrumentation Engineering 3, no. 8 (2014): 10963-10971.
- [4] Singh, Bhim, and Sanjeev Singh. "State of the art on permanent magnet brushless DC motor drives." journal of power electronics 9, no. 1 (2009): 1-17.
- [5] Lazor, Marek, and Marek Štulrajter. "Modified field oriented control for smooth torque operation of a BLDC motor." In 2014 ELEKTRO, pp. 180-185. IEEE, 2014.
- [6] John, Joseph P., S. Suresh Kumar, and B. Jaya. "Space vector modulation based field oriented control scheme for brushless DC motors." In 2011 International Conference on Emerging Trends in Electrical and Computer Technology, pp. 346-351. IEEE, 2011.
- [7] Li, Bo, and Chen Wang. "Comparative analysis on PMSM control system based on SPWM and SVPWM." In 2016 Chinese Control and Decision Conference (CCDC), pp. 5071-5075. IEEE, 2016.
- [8] Ting, Naim Suleyman, Yusuf Yasa, Ismail Aksoy, and Yakup Sahin. "Comparison of SVPWM, SPWM and HCC control techniques in power control of PMSG used in wind turbine systems." In 2015 Intl Aegean Conference on Electrical Machines & Power Electronics (ACEMP), 2015 Intl Conference on Optimization of Electrical & Electronic Equipment (OPTIM) & 2015 Intl Symposium on Advanced Electromechanical Motion Systems (ELECTROMOTION), pp. 69-74. IEEE, 2015.
- [9] Yun, Si Young, Ho Joon Lee, Jung Ho Han, and Ju Lee. "Position control of low cost brushless DC Motor using Hall sensor." In 2012 Sixth International Conference on Electromagnetic Field Problems and Applications, pp. 1-4. IEEE, 2012.

- [10] Ganesh, Chandramouleeswaran, and Sanjib Kumar Patnaik. "A simple first order compensator for brushless direct current drive based position control system." *Journal of Vibration and Control* 21, no. 4 (2015): 647-661.
- [11] Gamazo-Real, José Carlos, Ernesto Vázquez-Sánchez, and Jaime Gómez-Gil. "Position and speed control of brushless DC motors using sensorless techniques and application trends." *sensors* 10, no. 7 (2010): 6901-6947.
- [12] Sharma, Pragati K., and A. S. Sindekar. "Performance analysis and comparison of BLDC motor drive using PI and FOC." In *2016 International Conference on Global Trends in Signal Processing, Information Computing and Communication (ICGTSPICC)*, pp. 485-492. IEEE, 2016.